Energy Reports 15 (2026) 109387

Contents lists available at ScienceDirect

Energy Reports

journal homepage: www.elsevier.com/locate/egyr

Research paper

Enhanced microgrid management using sliding mode control with blockchain-enabled smart contracts for uncertainty regulation

Abdullah Umar [a], Rajdip Debnath [b], Deepak Kumar [b], Gauri Shanker Gupta [b], Vijayakumar Gali [c], Kashif Khan [a], Prashant K. Jamwal [a,*]

[a] Department of Electrical & Computer Engineering, Nazarbayev University, Astana, Kazakhstan
[b] Department of Electrical & Electronics Engineering, Birla Institute of Technology – Mesra, Ranchi 835215, India
[c] Department of Electrical & Electronics Engineering, School of Physics, Engineering, and Computer Science, University of Hertfordshire, Hatfield, United Kingdom

ARTICLE INFO

Keywords:
Blockchain
Smart Home Energy Systems
IoT Devices
Sliding mode control (SMC)
Prosumers
And Smart Contracts

ABSTRACT

This paper presents an integrated control and transactional framework aimed at enhancing the stability, resilience, and automation of decentralized microgrid systems. The proposed approach combines an advanced Sliding Mode Control (SMC) scheme with blockchain-enabled smart contracts to address critical challenges associated with conventional control strategies, including slow convergence rates, susceptibility to disturbances, and limited scalability. The SMC is augmented with a nonlinear disturbance observer to provide fast transient response, robust disturbance rejection, and reduced control chattering under dynamic operating conditions. A closed-loop interaction between the SMC and blockchain layers enables continuous two-way communication. Real-time operational parameters, such as power imbalances, voltage deviations, and frequency fluctuations, are transmitted from the controller to the blockchain layer. In response, smart contracts autonomously trigger control adjustments and Demand Response (DR) actions, which are fed back to the SMC as reference inputs. This dynamic feedback loop enables the system to adapt to fluctuations and uncertainties in both energy generation and consumption, thereby ensuring consistent power quality and system stability. Experimental results confirm the system's ability to maintain stability and improve power quality under varying operational conditions. Moreover, the system facilitates coordinated energy exchange among interconnected microgrids, thereby supporting the integration of local renewable energy sources and reducing dependence on centralized grid infrastructure.

1. Introduction

The transition toward sustainable energy systems is essential to address rising electricity demand, increase renewable energy integration, and improve the resilience and efficiency of modern power networks. Traditional centralized grids are often characterized by operational inefficiencies, high costs, and vulnerability to disturbances, limiting their suitability for increasingly distributed energy systems. At the same time, the rapid growth of smart home energy systems, IoT-enabled devices, and industrial electronics has increased the need for advanced local energy-management solutions (Pandiyan et al., 2024), (Yuan et al., 2025). Recent developments in blockchain-based secure architectures have further improved system transparency, trust, and protection against cyber threats (Sun et al., 2021). Microgrids offer a promising decentralized solution by enabling localized energy management and facilitating the integration of renewable energy sources, such as solar and wind. However, their operation is challenged by renewable intermittency, load uncertainty, and the need to maintain stable performance under dynamic conditions (Junaidi et al., 2023). In this regard, sliding mode control (SMC) is well-suited for microgrid applications because of its robustness against uncertainties and disturbances. The integration of nonlinear disturbance observers can further improve control accuracy, disturbance rejection, and chattering reduction. Motivated by these challenges, this work explores integrating observer-based SMC with blockchain-enabled smart contracts to enhance microgrid management. The proposed framework combines robust control performance with secure, transparent, and decentralized coordination to provide a resilient, scalable, and autonomous solution for uncertainty regulation and adaptive demand response in localized energy systems.

* Corresponding author.
E-mail address: prashant.jamwal@nu.edu.kz (P.K. Jamwal).

https://doi.org/10.1016/j.egyr.2026.109387
Received 25 December 2025; Received in revised form 23 March 2026; Accepted 9 May 2026
Available online 22 May 2026

In microgrid systems, inverters play a critical role in maintaining voltage and frequency control. Various control strategies, such as droop control and Virtual Synchronous Generator (VSG) schemes (Chen et al., 2023), have been implemented for parallel-connected inverters. Enhancements to droop control include proportional-integral terms to improve power controllability, while VSG controllers enhance steady-state regulation and transient response (Loh and Holmes, 2005). However, traditional multi-loop control structures often neglect the inner-loop dynamics, resulting in performance limitations. Voltage-controlled inverters typically use nested-loop control structures, comprising an outer voltage control loop and an inner current control loop to ensure reference tracking and dynamic compensation (Tian et al., 2023; Bharatee et al., 2023). Despite their prevalence, these structures often suffer from long transient responses and voltage deviations during load or reference variations. Advanced control strategies have emerged to address these limitations. Methods such as Deadbeat Control (Song et al., 2016), Finite Time Model Predictive Control (Shan et al., 2018), and Nonlinear Model-Based Control (Zhao et al., 2022) offer improved performance but are sensitive to model uncertainties and parameter perturbations, necessitating additional complexity in the form of disturbance observers or state compensators. Traditional control strategies, particularly those based on PI controllers, struggle with managing disturbances and parameter variations. Moreover, they introduce complexities such as phase-locked loops (PLLs) and filtering, which can slow system dynamics and exacerbate instability (Behera and Pattnaik, 2023). Furthermore, dual current controllers and cross-coupling between the d- and q-current components complicate the control structure. To tackle these challenges, innovative control strategies have been developed. SMC has shown particular promise due to its robustness, rapid dynamics, and disturbance rejection capabilities (Martins et al., 2019). However, conventional SMCs aim for sliding-mode variable convergence to zero, which requires high switching control gains and results in chattering (Alipour et al., 2023). Previous solutions using saturation or higher-order functions to reduce chattering have compromised the Lyapunov stability of SMC (Long et al., 2023), (Gui et al., 2021), (Shen et al., 2020), and (Zheng et al., 2018).

Blockchain technology significantly supports the management of regulatory uncertainty in microgrid energy trading through several key mechanisms. Transparency and trust are fundamental benefits of blockchain, as it provides a transparent ledger that records all transactions (Musleh et al., 2019) and (Islam et al., 2024). This transparency allows all participants in the microgrid network to view and verify transactions, fostering trust. With every transaction being publicly accessible and verifiable, the risk of fraud or manipulation is minimized, which is crucial for maintaining confidence in a decentralized energy trading system. The security and immutability of blockchain ensure that once transactions are recorded, they cannot be altered or deleted. This immutability is vital for maintaining the integrity of transaction records, ensuring that all data related to energy trading is secure and reliable. This security feature is particularly important in managing uncertainties, as it guarantees that the historical data used for forecasting and decision-making is accurate and tamper-proof (Golyan et al., 2024), (Danzi et al., 2017), and (Mumtaz et al., 2017). Decentralization is another significant advantage of blockchain. Operating on a decentralized network of nodes eliminates the need for a central authority, enhancing the resilience and reliability of the microgrid energy trading system. Even if some nodes go offline, the network continues to function, ensuring continuous operation and reducing the risk of single points of failure. Smart contracts are a key feature of blockchain technology that facilitates uncertainty management in microgrid energy trading. By automatically enforcing predefined conditions, smart contracts ensure transactions are executed efficiently and without intermediaries, reducing transaction costs and processing times (Chi et al., 2023), (Sivianes et al., 2023). This automation helps manage uncertainties by providing a predictable and reliable mechanism for energy trading.

Table I
Comparative analysis of the proposed SMC with blockchain approach to other prominent techniques.

Control Method	Advantages	Disadvantages	Proposed SMC with Blockchain – Comparative Benefits
Fuzzy-Based Control (Ranjan Das et al., 2024)	Simple implementation, suitable for basic stability control in microgrids.	Limited adaptability to real-time grid changes; poor disturbance rejection and slow response times; and a lack of a secure, decentralized framework.	Provides real-time adaptability, fast response, and blockchain-based security for P2P trading.
Passivity Fractional-Order SMC (Long et al., 2023)	Improved robustness; moderate response times under stable conditions.	High computational demand limits real-time applications; lacks scalability for large networks; no blockchain integration for secure transactions.	Achieves fast response with low computational complexity; blockchain enhances scalability and security.
Predictive Control with Private Blockchain (Danzi et al., 2017), (Sivianes et al., 2023), (Yu et al., 2023b)	Supports automated DR with basic security and improved energy management.	Centralized design limits scalability and flexibility; it lacks transparent P2P trading and a secure, public blockchain.	Decentralized, transparent P2P energy trading with Polygon Layer 2 blockchain; superior scalability.
Distributed Control with Cooperative Agents + Hybrid Blockchain (Yu et al., 2023a), (Li et al., 2024), (Yu et al., 2023b)	Decentralized, resilient framework with moderate transaction scalability.	High complexity; limited adaptability for high-frequency control; a blockchain hybrid may lack cost efficiency.	Lower complexity with adaptive SMC; enhanced real-time adaptability and economic efficiency.

Moreover, smart contracts enable dynamic pricing and load balancing. They can adjust energy prices in real time based on supply and demand, helping balance the load and optimize resource utilization within and between microgrids.

Additionally, during peak demand periods or energy shortages, smart contracts can automatically activate DR programs, incentivizing participants to reduce consumption or shift it to off-peak times. This proactive management of energy resources helps mitigate the uncertainties associated with variable energy generation and consumption. The proposed nonlinear observer-based adaptive SMC controller offers significant improvements, as shown in Table I.

First, it resolves the chattering issue by ensuring that the control gain exceeds the disturbance derivative boundary and applying disturbance compensation techniques using nonlinear disturbance observers. Second, it addresses the challenge of balancing disturbance approximation speed and sensor noise sensitivity by dynamically adjusting gains: a rapidly increasing control gain during the transient phase and a quickly diminishing gain during the steady state to alleviate chattering. By integrating the robust control capabilities of SMC with the security and transparency of blockchain, this approach optimizes microgrid performance, manages uncertainties, and improves local energy generation, reducing reliance on the main grid. In Fig. 1, the local microgrid controller processes data from PV systems, BESS, and loads, and

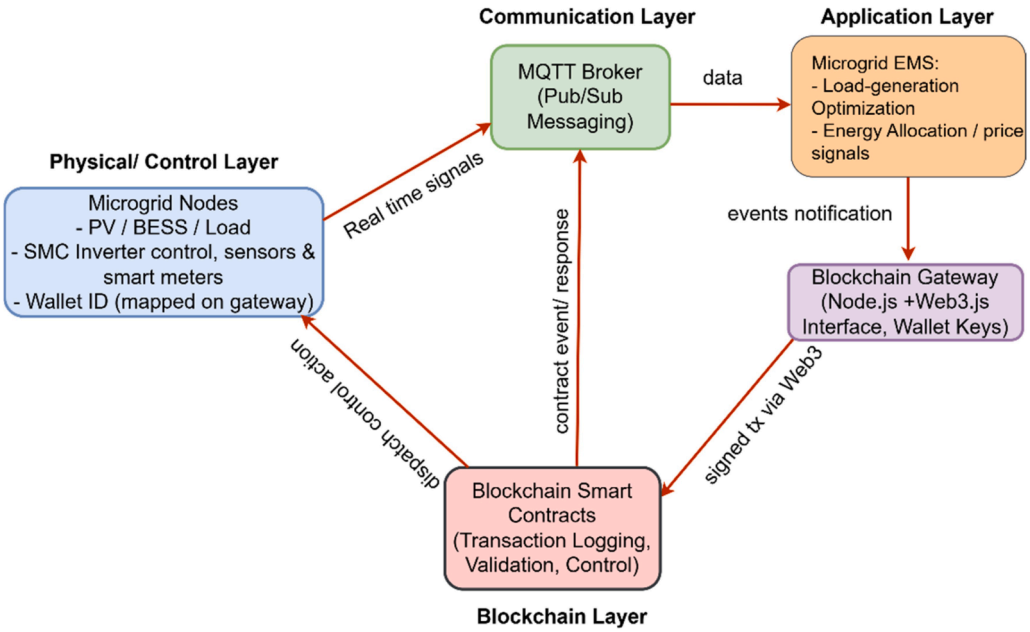

Fig. 1. Observer-based sliding mode controller with blockchain-enabled EMS for real-time demand response and adaptive microgrid control.

transmits real-time operational parameters (e.g., active power, frequency, voltage deviations) to the microgrid control center. The energy management system (EMS) in the control center optimizes load generation and communicates with a smart contract layer on the blockchain to trigger demand response (DR) actions. The resulting demand response setpoints are sent back to the local inverter controller for real-time actuation, forming a cyber-physical feedback loop for secure and adaptive microgrid operations. The decentralized nature of blockchain promotes energy independence and resilience, as microgrids can operate autonomously or in cooperation with neighboring microgrids, creating a flexible and adaptable energy ecosystem.

Major Contributions:

- Stability via Adaptive SMC & Blockchain: Introduces an adaptive sliding mode control (SMC) with nonlinear observer and blockchain smart contracts to enhance microgrid stability, minimize chattering, and ensure robustness under disturbances.
- Reliable Power & Fault Management: Proposes a macro-variable-based SMC ensuring balanced power sharing and finite-time convergence, preventing inverter faults and load shedding.
- Automated Real-Time Demand Response: Embeds DSM logic into smart contracts for autonomous, real-time voltage/frequency-based demand response, improving grid resilience and reducing manual control.
- Scalable Blockchain-Enabled Operation: Leverages Polygon Layer 2 blockchain for low-cost, high-speed P2P energy trading and DR execution in large-scale, interconnected microgrid systems.

1.1. The paper is organized as follows

Section II explains the design of the SMC, detailing the control strategy and its enhancements for improved disturbance handling and stability. Section III covers the implementation of blockchain technology, describing the development and use of smart contracts on the Ethereum platform to enable secure and decentralized P2P energy trading and DR programs. Section IV presents the results and discussion, showcasing simulations and hardware-in-the-loop experiments that validate the system's performance and highlight improvements in stability, efficiency, and reliability. Finally, Section V concludes the paper by summarizing key findings and contributions, and by suggesting areas for future research, emphasizing the importance of integrating SMC and blockchain for advanced microgrid management and sustainability.

2. Microgrid system modeling and proposed control laws

The proposed SMC controller uses a multi-layer structure: an inner current control SMC loop, a middle voltage control SMC loop, and an outer power control SMC loop, all coordinated via the observer. The controller rapidly adjusts the inverter's output to maintain voltage stability and power balance. The overall control diagram and SMC control law schematic are depicted in Figs. 3 and 4, respectively, highlighting how the loops interact. This control strategy maintains stable voltage and frequency in the microgrid and shares power according to setpoints, even under disturbances like sudden load changes or inverter faults. The microgrid's inverter-based generation system is modeled as a nonlinear system with parametric uncertainties and external disturbances. Nonlinear systems with variable degrees of uncertainty can be represented as:

$$\dot{x} = Ax + £(y,u) + B(t,y,u)\varphi + D\mathrm{w}(t) \tag{1}$$

$$y = Cx \tag{2}$$

where the system states, output, and controllable input are given by the vectors $x \in \Re^n$, $y \in \Re$ and $u \in \Re^m$ respectively. $\varphi \in \Re$ denotes parameters that are unknown and $\mathrm{w} \in \Re$. These are the external disturbances. It is further recognized that the functions B and φ guarantee unique solutions $(x(t, \quad t_0, x_0))$ to system (1) for all permissible errors/disturbances for an initial condition x_0 at time t_0. The intended objective is to produce estimates of the state and the unknown parameter φ, by relying only on data from y, the output, and dampening the impact of w, the external disruptions.

2.1. A. Nonlinear observer design

Nonlinear observer design estimates the state of an unobservable system (Martins et al., 2019). The nonlinear observer design can be implemented as:

$$\dot{\hat{\varphi}} = (A - KC)\hat{\varphi} + B(t,y,u) \tag{3}$$

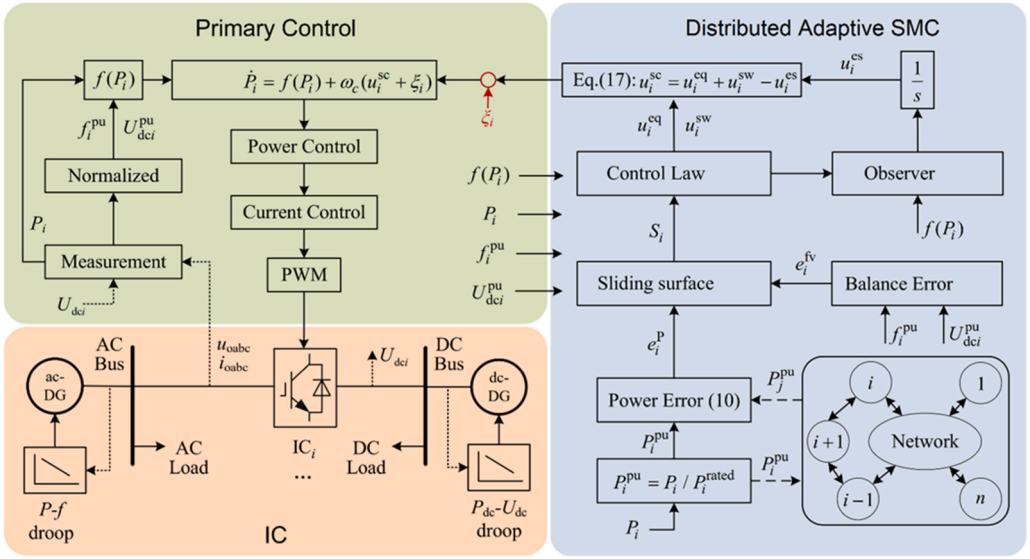

Fig. 2. Schematic of the overall control diagram.

$$\dot{\hat{\theta}} = \Gamma \mathbb{P}^T C^T \lceil y - C\dot{x} \rfloor^{\alpha} \tag{4}$$

$$\hat{x} = z + T^{-1} v \tag{5}$$

$$\dot{z} = Az + £(y,u) + B(t,y,u)\hat{\theta} + K(y - Cz) + \mathbb{P}\dot{\hat{\theta}} \tag{6}$$

$$\dot{\epsilon} = A_0 \epsilon + a(y - Cz) + \aleph(\epsilon_1, y - Cz) \tag{7}$$

where, $\hat{x}$, $\hat{\theta} \in \Re^n$ and z denotes the estimated vectors and state estimator, respectively. The error dynamics of the state estimation is given by ϵ. $\mathbb{P} \in \Re^n$ is a supplementary variable. Eq. (4) characterizes the nonlinear dynamics of the model parameter estimation in terms of $\alpha = 0$ for discretized domain, $\alpha = 1$ for linearized domain and $\alpha \in (0, 1)$ for continuous domain analysis. The observer gain is denoted as $K \in \Re^n$ and T is the transformation matrix. The nonlinear perturbation $\aleph \in \Re * \Re \rightarrow \Re^n$ can be characterized as:

$$\aleph(\epsilon_1, y - Cz) := \begin{bmatrix} k_1 \lceil (y - Cz) - \epsilon_1 \rfloor^{\frac{n-1}{n}} \\ k_2 \lceil (y - Cz) - \epsilon_1 \rfloor^{\frac{n-2}{n}} \\ \vdots \\ k_n \lceil (y - Cz) - \epsilon_1 \rfloor^{0} \end{bmatrix} \tag{8}$$

2.2. B. SMC-sliding manifold design and stability laws

Sliding manifold design and stability laws are key components of SMC (Shan et al., 2018) and (Alipour et al., 2023). The reaching law drives the state/error trajectory to the sliding manifold, and the control law maintains that trajectory on the manifold. The nonlinear uncertain system is asymptotically stable in the sliding manifold defined by:

$s = z_1 + \sum_{i=1}^{n-2} c_i z_{i+1} + z_n$ (s=Hurwitz for all $c_i > 0$) (9)

The Lyapunov stability of the sliding manifold can be defined by a function:

$$V = \zeta^T P \zeta + \frac{1}{2}\left(\tilde{\theta}_1^2 + \tilde{\theta}_2^2 + \ldots + \tilde{\theta}_{n-2}^2 + \tilde{\theta}_{n-1}^2\right) \tag{10}$$

The time derivative of V along the trajectory of error dynamics:

$$\dot{V} = -s^{-\frac{1}{\rho}} \zeta^T P \zeta \leq 0 \tag{11}$$

where P = positive definite and symmetric and $\dot{\tilde{\theta}}_1 = -k\phi^{(n-1)}(z_1) \ldots \dot{\tilde{\theta}}_{n-2} = -k\phi^{(2)}(z_1)$, $\dot{\tilde{\theta}}_{n-1} = -k\phi^{(1)}(z_1)$ and $k = 2y|s|^{-\frac{1}{\rho}}(k_1 s^{\gamma} \mathrm{sign}(s) + k_2 w)$

The proposed sliding-mode-based controller for inverter-based resources achieves multiple control objectives, including power and current tracking and DC-link voltage regulation. By rapidly switching between control modes, the controller maintains the system on the sliding manifold, ensuring convergence to the intended state. The control diagram (Fig. 2) and schematic of the control laws (Fig. 3) illustrate the key features.

2.3. C. Active and reactive power control loop

To guarantee that the P and Q tracking errors converge to specified boundaries in a finite time, an enhanced SMC is proposed here. The dynamics of the overall controller loops are as follows:

$$\dot{i}_{\alpha\beta} = \frac{v_{\alpha\beta}}{L} - \frac{x_1 u_{\alpha\beta}}{2L} + \frac{x_2}{\sqrt{3}L}\begin{bmatrix} \frac{1}{2\sqrt{2}}\left(u_\beta^2 - u_\alpha^2\right) - u_\alpha u_\gamma \\ \frac{1}{\sqrt{2}} u_\alpha u_\beta - u_\beta u_\gamma \end{bmatrix} \tag{12}$$

$$\dot{v_{dc}} = u_{\alpha\beta}^T i_{\alpha\beta} \Big/ \mathrm{C} - 2v_{dc}/RC = \dot{v_{dc1}} + \dot{v_{dc2}} \tag{13}$$

$$\dot{x}_1 = \frac{u_{\alpha\beta}^T i_{\alpha\beta}}{C} - \frac{2x_1}{CR} \tag{14}$$

$$\dot{x}_2 = \frac{2u_{\alpha\beta}^T i_{\alpha\beta} u_\gamma}{\sqrt{3}C} + \frac{1}{\sqrt{6}C}\left(\left(u_\alpha^2 - u_\beta^2\right) i_\alpha - 2u_\alpha u_\beta i_\beta\right) \tag{15}$$

where the vector data of the phase current and grid voltage in $\alpha\beta$ reference frame are denoted by $i_{\alpha\beta} = \left[i_\alpha, \; i_\beta\right]^{\mathrm{T}}$ and $v_{\alpha\beta} = \left[v_\alpha, v_\beta\right]^{\mathrm{T}}$ respectively. The dc link voltage is represented as $v_{dc}(x_1 = V_{dc1} + V_{dc2}; x_2 = V_{dc1} - V_{dc2})$ and the average duty cycle vectors are given by $u_\alpha u_\beta u_\gamma =$ $\left[u_\alpha, u_\beta, u_\gamma\right]^{\mathrm{T}}$.The control action also facilitates the P and Q injections which can be represented as:

$$p = v_\alpha i_\alpha + v_\beta i_\beta \tag{16}$$

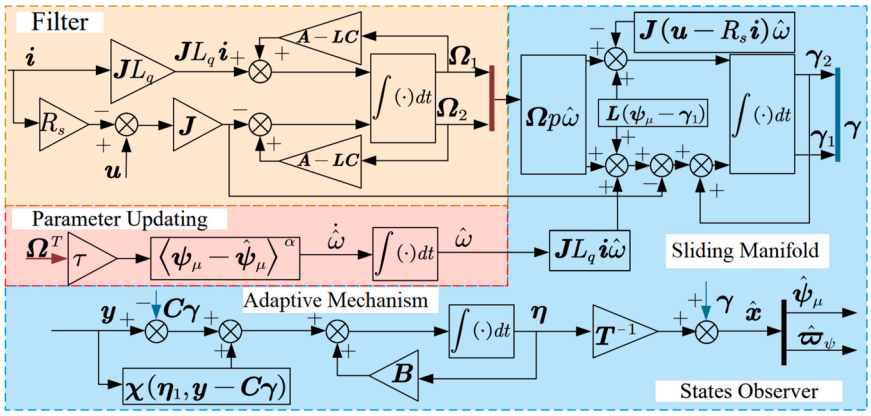

Fig. 3. Schematic of the proposed SMC control laws.

$$q = v_\alpha i_\beta - v_\beta i_\alpha \tag{17}$$

$$\dot{p} = \frac{1}{L}\|v_{\alpha\beta}\|^2 - \frac{1}{2L}x_1 v_{\alpha\beta}^T u_{\alpha\beta} + \omega q \tag{18}$$

$$\dot{q} = -\frac{1}{2L}x_1 \left(Jv_{\alpha\beta}\right)^T u_{\alpha\beta} - \omega p \tag{19}$$

where, ω is the grid angular frequency and $J = \begin{bmatrix} 0 & -1 \\ 1 & 0 \end{bmatrix}$. The tracking error dynamics as well as the sliding manifolds are described as:

$$e_p = p^\star - p,\ e_q = q^\star - q \tag{20}$$

$$s_{SMCp} = k_{pSMC}e_p, \quad s_{SMCq} = k_{pSMC}e_q \tag{21}$$

$k_{pSMC}$is a constant, whereas the reference values are $p^\star$ and $q^\star$. The derivative of $e_p$and e_q following the error dynamics trajectory over time are obtained:

$$\dot{e}_p = -\frac{1}{L}\|v_{\alpha\beta}\|^2 + \frac{1}{2L}x_1 v_{\alpha\beta}{}^T u_{\alpha\beta} - \omega q + \mathrm{w}_p \tag{22}$$

$$\dot{e}_q = \frac{1}{2L}x_1 \left(Jv_{\alpha\beta}\right)^T u_{\alpha\beta} + \omega p + \mathrm{w}_q \tag{23}$$

where, $\mathrm{w}_{pq} = [\dot{p^\star}\ \dot{q^\star}]^T$ represents external disturbances. As a result, the power control loop's tracking error dynamics are constrained by the sliding manifold as:

$$u_{\alpha\beta} = u_{\alpha\beta}^{eq} - \mu(e_p)v_{\alpha\beta} - \mu(e_q)Jv_{\alpha\beta} \tag{24}$$

$$u_{\alpha\beta}^{\mathrm{eq}} = \frac{2}{x_1\|v_{\alpha\beta}\|^2}\left[\left(\|v_{\alpha\beta}\|^2 + L\omega q\right)v_{\alpha\beta} - L\omega p Jv_{\alpha\beta}\right] \tag{25}$$

where the steady state equilibrium condition $u_{\alpha\beta}^{\mathrm{eq}}$ is generated after equating $\dot{p}$, $\dot{q} = 0$. Similarly, for the *current control loop*, the tracking error dynamics of the observer can be defined as:

$$\dot{\tilde{i}}_{\alpha\beta} = -\lambda_{\alpha\beta}\left|\tilde{i}_{\alpha\beta}\right|^{\frac{1}{2}}\mathrm{sign}\left(\tilde{i}_{\alpha\beta}\right) + \phi_{\alpha\beta} \tag{26}$$

$$\dot{\phi}_{\alpha\beta} = -\varphi_{\alpha\beta}\mathrm{sign}\left(\tilde{i}_{\alpha\beta}\right) + \dot{\widetilde{\mathrm{w}}}_{\mathrm{d}\alpha\beta} \tag{27}$$

The SMC power controller applies corrections to the inner-loop reference signals (voltage or current) so that any deviation in output power (due to load changes or faults) is swiftly corrected. The error dynamics for power and current loops are formulated and shown to be globally bounded on their respective sliding surfaces. By properly

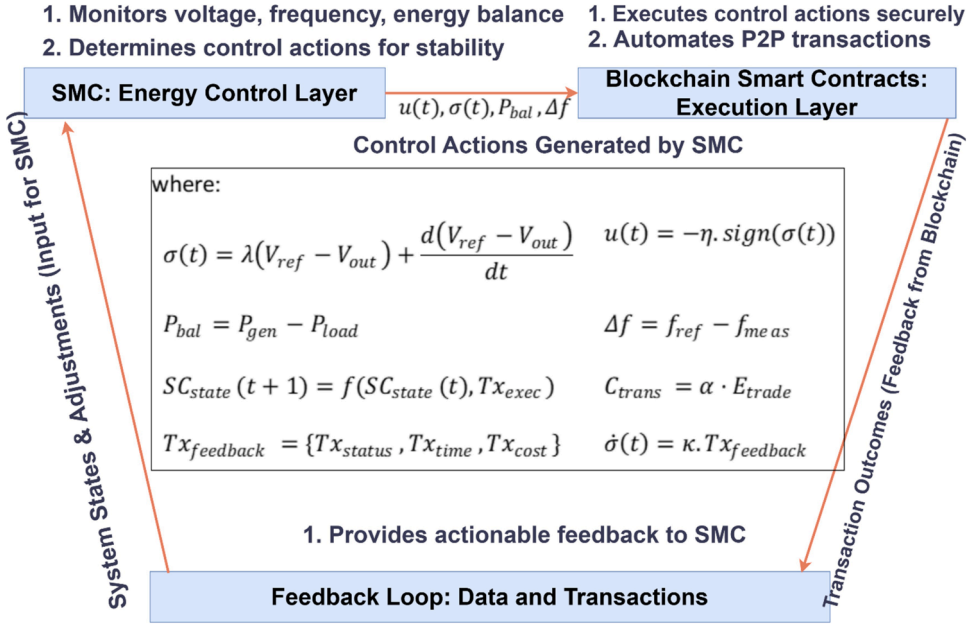

Fig. 4. Interaction dynamics between the sliding mode controller (Smc) and blockchain-enabled smart contracts.

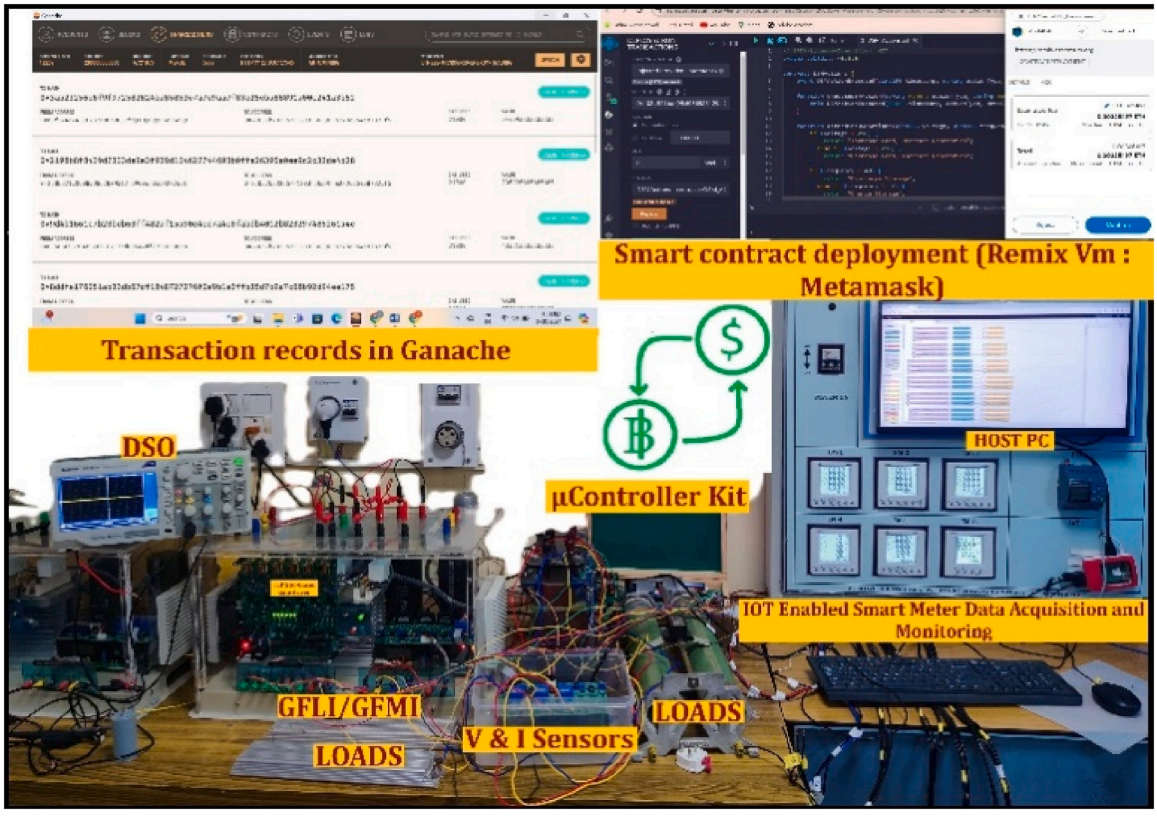

Fig. 5. Experimental Setup for the proposed design framework.

selecting gains and reaching laws, we ensure that the tracking errors for active power P and reactive power Q are driven to a neighborhood of zero in finite time, thereby achieving near-instantaneous power-sharing adjustments among inverters.

3. Blockchain smart contracts design under uncertainty regulation

The proposed framework establishes a seamless integration between the Sliding Mode Control (SMC) system and blockchain-enabled smart contracts, forming a closed-loop interaction between the physical and cyber layers of the microgrid. In this design, the SMC controller is responsible for maintaining voltage and frequency stability and managing active and reactive power flows in response to system dynamics and disturbances. Simultaneously, blockchain smart contracts govern decentralized energy trading and demand response (DR) by executing validated peer-to-peer transactions among microgrid participants. The connection between the two components is realized through real-time data exchange: the SMC continuously monitors parameters such as power surplus or deficit, frequency deviations, and voltage variations, and relays these measurements as input signals to the blockchain layer. Smart contracts utilize this control-side information to automate trading decisions or trigger DR events, ensuring energy balance and system reliability. Once a trade is executed or a DR event is initiated on the blockchain, the resulting transaction data, such as updated energy allocations, target power setpoints, and curtailment commands, is transmitted back to the controller as reference signals. The SMC then adapts its control actions accordingly to enforce these decisions at the physical level, ensuring that the outcomes of smart contract logic are reflected in real-world power flows. This bidirectional communication enables a fully autonomous, adaptive microgrid system in which secure energy transactions and control stability are co-optimized in real time.

Figs. 3 and 4 illustrates the vital interplay between the Sliding Mode Controller (SMC) and Blockchain Smart Contracts in achieving decentralized microgrid management. This interaction establishes a closed-loop system in which robust control dynamics are tightly coupled with secure, decentralized transaction processing to enhance the microgrid's operational stability and transparency. The SMC generates control signals, denoted by $u(t)$, which are computed based on the deviation between the reference voltage V_{ref} and the actual voltage output V_{out}, captured through the sliding surface $\sigma(t)$. These control signals, along with key state variables such as power balance P_{bal} and frequency deviation Δf, are transmitted to the blockchain layer for secure execution.

Upon receiving these control inputs, the blockchain smart contract enforces predefined operational rules in a tamper-proof, transparent manner. This includes validation of energy balance constraints and associated transaction costs, thereby maintaining system integrity while supporting decentralized decision-making. The smart contracts process energy trading and operational commands, generating feedback outputs such as transaction status Tx_{status}, energy balance verification E_{bal}, and incurred transaction costs C_{trans}. These outputs are sent back to the control layer, enabling the SMC to incorporate real-time transaction outcomes into its control decisions. The feedback mechanism facilitates adaptive control by dynamically updating the sliding surface $\sigma(t)$ and its derivative $\dot{\sigma}(t)$, thereby refining the control signal $u(t)$, to ensure system stability. If the blockchain feedback indicates transaction failures, imbalance in generation and demand, or rising transaction costs, the SMC adjusts its control strategy to compensate for these deviations. This bidirectional integration ensures that the microgrid remains resilient, maintains voltage and frequency stability, and operates efficiently under diverse operational conditions, including faults or sudden demand shifts.

In smart home energy systems using IoT devices (Mumtaz et al., 2017), efficient energy management is crucial. The Microgrid Operator analyzes data to determine the optimal energy distribution strategy, taking into account energy demand, supply, and storage levels. During

high demand, non-critical loads are reduced or shifted to off-peak periods, and microgrids are incentivized to increase production or release stored energy. The challenge is to optimize resource use to minimize costs while maintaining stability and efficiency (Chi et al., 2023). This involves complex decisions on when to generate, store, or consume energy based on local demand, renewable availability, and storage levels. Without a main grid connection, balancing generation and consumption within and between microgrids is crucial to prevent outages. Blockchain technology enhances coordination by providing a secure, transparent platform for P2P energy trading and demand response, which can be seamlessly integrated into smart home systems. Decentralized decision-making allows each microgrid to manage its resources while contributing to overall system efficiency. The contracts manage the automatic adjustment of energy consumption in response to grid signals or market prices. For example, during peak demand periods, the contract can trigger load reductions by temporarily turning off non-essential appliances or by shifting consumption to off-peak hours. Algorithm 1 outlines a blockchain-based energy trading process for DR activation. The consumer flexibility profiles are predefined in the contracts and can be dynamically adjusted based on real-time grid conditions. The system continuously monitors voltage and frequency levels within each microgrid.

Algorithm 1. Smart Contract for DR Program Activation

```
SmartContract_DR
procedure SmartContract_DR(voltage, frequency)
    if voltage < V_min or voltage > V_max or frequency < f_min or frequency > f_max then
        dsmActions = determineDSMActions(voltage, frequency)
        executeDSMActions(dsmActions)
        recordDSMActionsOnBlockchain(dsmActions)
    end if
end procedure
determineDSMActions
procedure determineDSMActions(voltage, frequency)
    actions = []
    if voltage < V_min then
        actions.append(reduceNonCriticalLoad())
        actions.append(increaseGeneration())
    else if voltage > V_max then
        actions.append(increaseNonCriticalLoad())
        actions.append(decreaseGeneration())
    end if
    if frequency < f_min then
        actions.append(dischargeStorage())
    else if frequency > f_max then
        actions.append(chargeStorage())
    end if
    return actions
end procedure
executeDSMActions
procedure executeDSMActions(dsmActions)
    for each action in dsmActions do
        performAction(action)
    end for
end procedure
recordDSMActionsOnBlockchain
procedure recordDSMActionsOnBlockchain(dsmActions)
    recordEventOnBlockchain(dsmActions)
end procedure
```

4. Results and discussions

This section presents a detailed analysis of both simulation and experimental validations. The performance of the proposed controller is thoroughly evaluated and benchmarked against two prominent alternatives: a conventional Sliding Mode Controller (SMC) using a sign-function-based sliding manifold with a disturbance observer, and a Proportional-Integral (PI) controller, widely adopted in industrial applications.

To validate the efficacy of the proposed SMC, a laboratory test setup was constructed as shown in Fig. 5. The test bed includes two 3.3 kVA three-phase VSCs, which can both act as either GFL/GFM inverters from SEMIKRON with local loads connected in parallel at the PCC, an auto-transformer, LEM current and voltage sensors for accurate measurements, a TLP 250-based gate driver circuit, and a programmable DC supply. The network and control settings follow those specified in Table II.

1) Case 1: Comparative Performance analysis against nonlinear loading conditions:

In Fig. 6, a graphical analysis of the efficacy of the proposed SMC in the context of harmonics rejection and robustness against nonlinear loading conditions. Turning our attention to the SMC's response to nonlinear loading conditions, we note a commendable level of robustness. As the loading conditions become increasingly nonlinear, characterized by rapid fluctuations and distorted waveforms, as indicated by the THD values, the SMC maintains a stable output current profile

Table II
System parameters.

Parameter	*Values*
Input voltage	750 V
Output voltage	380 V
Switching frequency	10 kHz
Filter L and C	2 mH and 10 micro-F
Output Power	6 kW
Sliding coefficients	K= 0.15
SMC-Current regulation loop	$\lambda_{cc} = 4000$, $\eta_{cc} = 2800$, $k_{cc} = 1000$, $\varepsilon_{cc}= 0.001$
SMC-Voltage regulation loop	$\lambda_{vc} = 1500$, $\eta_{vc} = 200$, $k_{vc}= 1000$, $\varepsilon_{vc} = 0.01$
SMC-Power regulation loop	$\lambda_{pc} = 2000$, $\eta_{pc} = 400$, $k_{pc} = 1000$, $\varepsilon_{pc} = 0.01$

compared to traditional SMC.

2) Case Study 2: Load variations (active power reference variation)

The proposed controller's robustness and performance were evaluated under load variations in grid-following and grid-forming inverters, highlighting its effectiveness for practical applications. Introducing load variations of 25%, the proposed controller demonstrated exceptional adaptability and responsiveness. It dynamically adjusted control loops to accommodate changing load conditions, maintaining stable voltage and frequency despite fluctuations. The system exhibited acceptable transient response and settling time, indicating efficient handling of load variations, which was also proved through experimental results in Fig. 7 (a) and (b), showing less tracking error dynamics.

3) Case Study 3: Grid harmonics rejection in case of sudden changes of grid impedance

Assessing the responsiveness of GFL and GFM inverters to rapid changes in grid impedance is a significant component of evaluating their performance. During a rapid variation in grid impedance of Lg= 6 mH (weak grid) and Lg= 12 mH (very weak), it significantly affects the stability and degradation in the power quality delivered to the connected loads whenever traditional control is applied, as can be seen in Fig. 8(a). In comparison, the performance analysis signifies that the proposed controller exhibits a high degree of robustness against changes in grid impedance, as can be seen from Fig. 8(b). The controller quickly adjusts the control loops to compensate for variations in grid impedance, ensuring accurate voltage and frequency regulation with minimal fluctuations and low overshoot, and a fast transient response, as illustrated and confirmed by experimental results.

4) Case Study 4: comparative analysis of the proposed controller with state-of-the-art controllers

Fig. 9 presents an experimental comparison, and Table III details the comparative performance analysis of three control strategies: fuzzy-based intelligent control (Ranjan Das et al., 2024), Passivity Fractional-Order Sliding-Mode Control (Long et al., 2023), and the proposed strategy combining Sliding Mode Control (SMC) with a nonlinear disturbance observer and blockchain technology. Table III shows that the proposed SMC with a blockchain framework provides the most balanced performance among the compared methods. In addition to achieving the lowest THD, overshoot, settling time, and steady-state error, it also offers stronger disturbance rejection and adaptability to grid distortions. Unlike the benchmark controllers, the proposed method further incorporates blockchain-enabled transparency, cybersecurity, and decentralized coordination, making it better suited to practical autonomous microgrid operation. Fig. 10 illustrates the experimental comparison between conventional fuzzy-based intelligent control (Ranjan Das et al., 2024) and the proposed strategy, which employs a nonlinear disturbance observer-based Sliding Mode Control (SMC) integrated with blockchain smart contracts. The results are captured

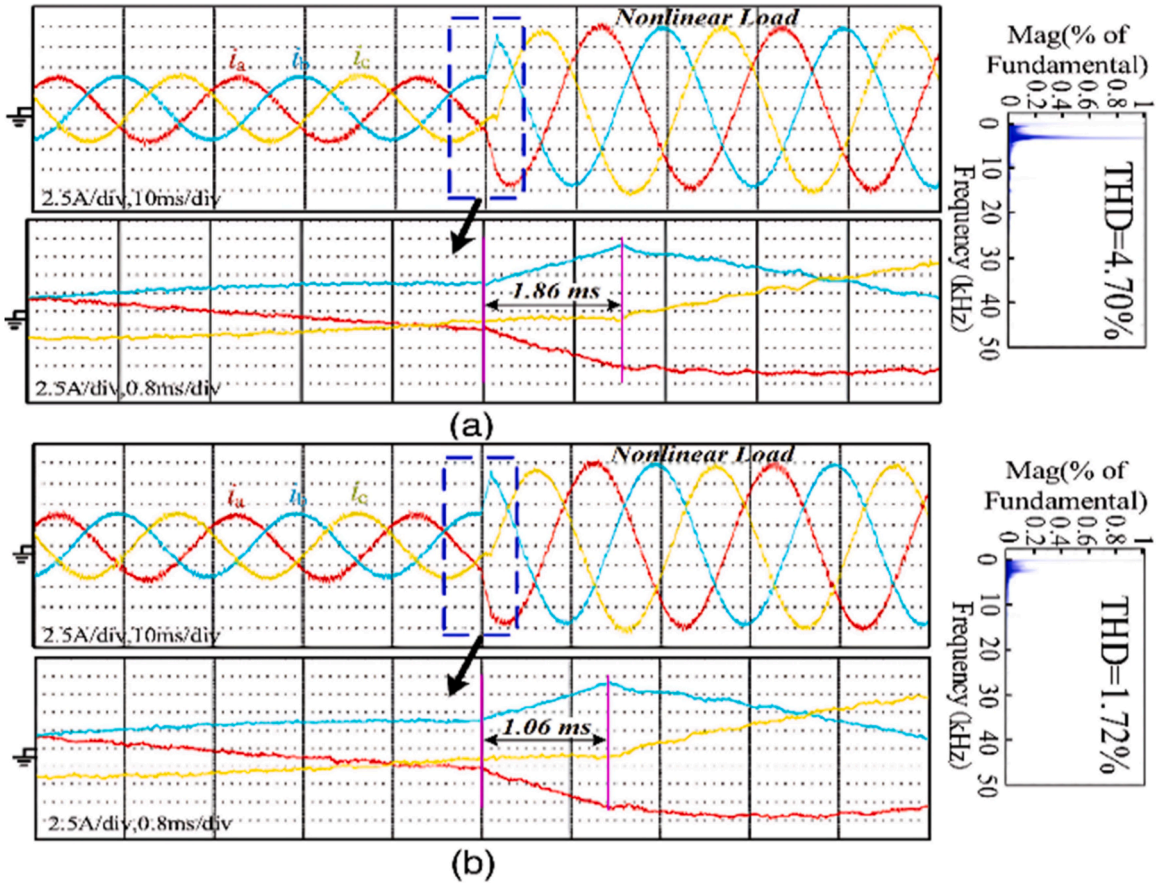

Fig. 6. Experimental waveforms during nonlinear loading (a) conventional SMC (b) proposed SMC.

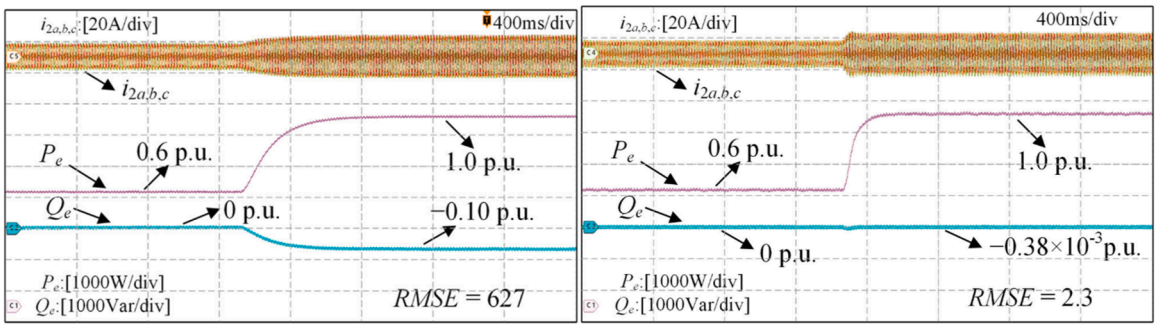

Fig. 7. Experimental comparative results (a) Traditional control (b) Proposed control.

within a single measuring window, with an intermediate variable for analysis. As shown in Fig. 10(a), when the a-phase and b-phase grid voltages decrease by 10% and 25%, respectively, the proposed strategy achieves a significant reduction in dc-link voltage ripple, highlighting its superior ability to handle voltage sags. In contrast, the fuzzy-based control method exhibits severe input current distortion, resulting in a maximum Total Harmonic Distortion (THD) of 31%. The proposed strategy, however, reduces the input current THD to an impressive 2.5%.

In Fig. 10 (b), under distorted grid conditions, the maximum input current THD using the fuzzy-based approach is 18%. Switching to the proposed strategy further reduces the input current THD to 2%, demonstrating its effectiveness in maintaining power quality even under non-ideal grid conditions. Furthermore, Fig. 10(c) shows that, with the fuzzy-based strategy, the input current THD spikes to 40% and a significant dc-link voltage ripple is observed. The proposed strategy effectively suppresses this ripple and reduces the input current THD to 2.1%, confirming its robustness against disturbances. Fig. 10 (d) and (e) further corroborate these findings, showing phase-voltage and current waveforms and FFT results of grid voltage and input current, respectively, demonstrating the superior harmonic-mitigation capabilities of the proposed strategy under unbalanced and distorted grid conditions. These results indicate that the improved performance is not limited to a single operating case but is maintained across unbalanced, distorted, and combined disturbance scenarios. This consistency confirms that the nonlinear disturbance observer enhances disturbance estimation, while the multiloop SMC structure improves tracking precision and dynamic regulation, leading to better waveform quality and harmonic suppression than the compared benchmark strategies. The proposed control strategy, which integrates a nonlinear disturbance observer-based Sliding Mode Control (SMC) with blockchain-enabled smart contracts, demonstrates significant performance enhancements over conventional methods such as fuzzy-based control, Passivity Fractional-Order SMC (FOSMC), droop control with virtual inertia, predictive control with a private blockchain, and conventional PI control. The experimental results, as summarized in Table III, underscore the advantages of the proposed approach in several critical areas.

Power Sharing Between the Microgrids and Blockchain Implementation: Table IV summarizes five representative scenarios in a blockchain-enabled microgrid hardware setup, demonstrating the interaction between energy exchange, SMC-based control, and system behavior. In Case 1, a low-load condition with high PV generation results in a 0.2 kW surplus, which is securely traded via smart contracts, with the SMC maintaining 98% tracking accuracy. Case 2 illustrates a high-load situation where a 1 kW deficit is covered through blockchain-mediated import, and the SMC ensures grid power matching with ±1% voltage regulation. Case 3 involves real-time fluctuations managed through dynamic P2P contracts updated every 200 ms, where the SMC adapts effectively, achieving over 90% improvement in power quality. Case 4 reflects an islanding condition with 3.2 kW demand met locally, and SMC enables a smooth transition with $\leq$ 1.5% voltage deviation. Finally, in Case 5, during a DR event, 2.5 kW is supplied through the prosumer network, and the SMC tracks DR-modified references with 94% accuracy. Across all cases, the integration of blockchain ensures secure transactions, while the SMC delivers stable and responsive control performance.

The results from Table V highlight significant advancements in the scalability and performance of blockchain networks, particularly with the integration of the Polygon network. The scalability improvements are evident with methods like Layer 2 rollups, which significantly increase transaction throughput and reduce latency compared to the base Ethereum network. For instance, while the base Ethereum network processes 30 transactions per second (TPS) with a 15-second latency, Polygon, as a Layer 2 solution, boosts throughput to between 2000 and 7000 TPS, with latency reduced to just 1–2 s. In parallel, the performance metrics for smart contracts in Table VI focus on optimizing execution time and gas costs within the Polygon network. Contracts designed for secure energy trading and demand response exhibit varying execution times and gas costs. For instance, the secure energy trading contract, despite its higher gas cost on the Ethereum main chain, benefits from Polygon's negligible transaction fees. Fig. 11 illustrates the

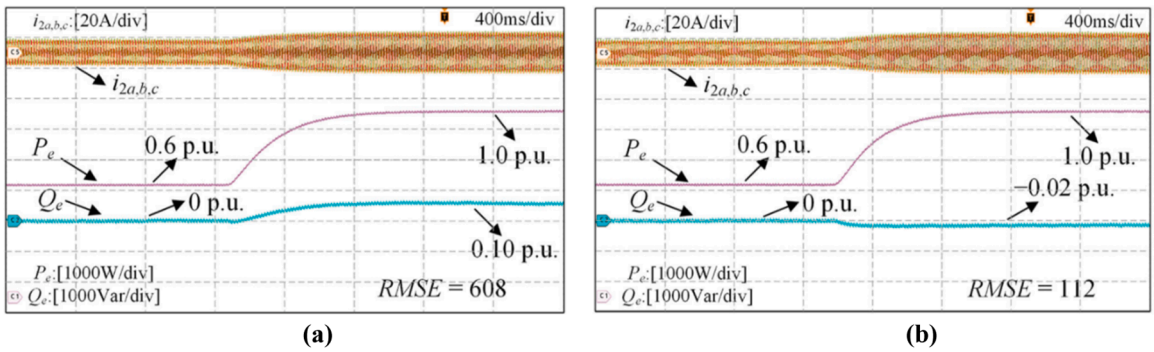

Fig. 8. Experimental comparative results under SCR variations (a) Traditional (b) Proposed.

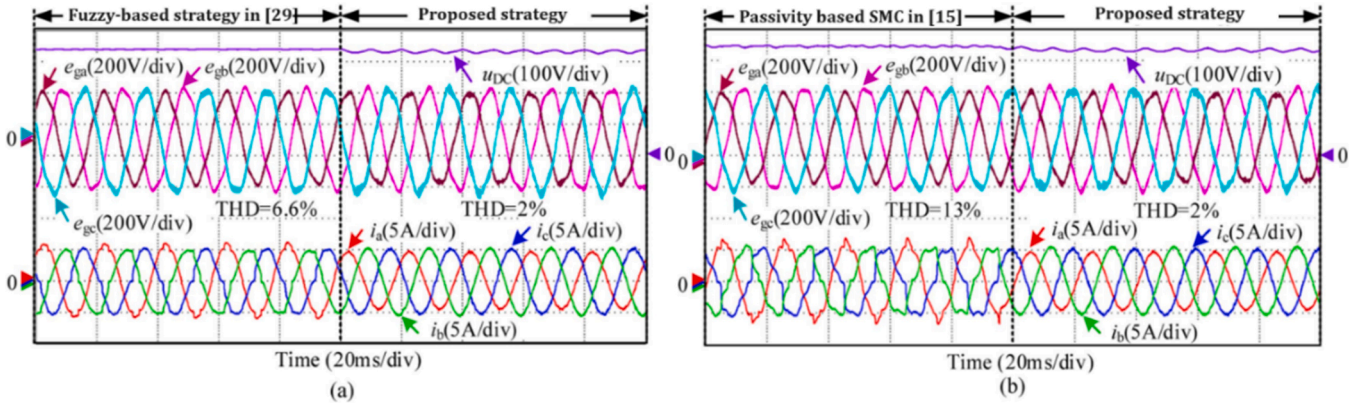

Fig. 9. Experimental comparison results between the state of the art and the proposed strategies. (a) fuzzy-based intelligent control in (Ranjan Das et al., 2024) (b) Passivity Fractional-Order Sliding-Mode Control in (Long et al., 2023).

Table III
A Comparative Analysis of the Performance Metrics of "Proposed SMC Controller with Blockchain" with Other Controllers.

Performance Metric	Proposed SMC + Blockchain	Fuzzy-Based Control Ranjan Das et al., (2024)	Passivity FOSMC Long et al., (2023)	Droop + Virtual Inertia	Conventional PI Control
Convergence Rate (ms)	< 10	~30	~15	~20	~35
Disturbance Rejection (Suppression)	High (95%)	Low (50%)	Moderate (75%)	Moderate (70%)	Low (45%)
Transaction Transparency	High (Blockchain Enabled)	Low	Moderate	None	None
Frequency Deviation Suppression (%)	95%	50%	75%	65%	40%
Power Quality Improvement (%)	90%	40%	70%	60%	35%
Total Harmonic Distortion (THD)	2%-2.5%	18%-40%	10%-15%	15%-20%	25%-30%
Overshoot (%)	Minimal (~2%)	High (~15%)	Moderate (~8%)	Moderate (~10%)	High (~20%)
Settling Time (ms)	< 8	~30	~15	~18	~35
Rise Time (ms)	< 5	~25	~12	~15	~30
Latency for Transactions (ms)	< 5	N/A	N/A	N/A	N/A
Scalability	High (Decentralized, P2P)	Low	Moderate	Low	Low
Cybersecurity	High (Blockchain Secured)	Low	Moderate	None	Low
Implementation Complexity	Moderate	Low	High	Low	Low
Computational Overhead	Moderate (Blockchain)	Low	High (Fractional Calculations)	Low	Low
Cost Effectiveness	High	High	Moderate	Low	High
Adaptability to Grid Distortions	High (Dynamic Compensation)	Low	Moderate	Low	Low
Steady-State Error (%)	~0.5%	~7%	~3%	~5%	~8%

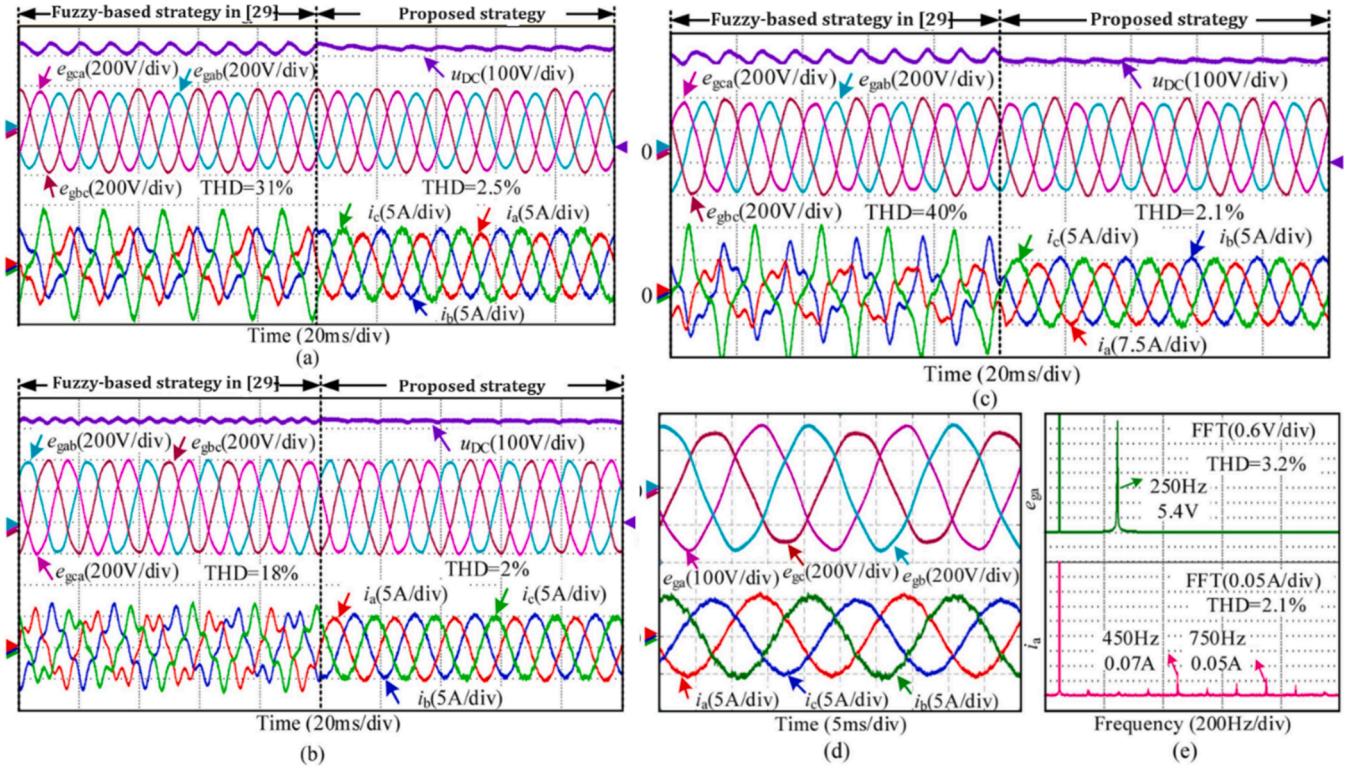

Fig. 10. Experimental comparison results between the fuzzy-based intelligent control in (Ranjan Das et al., 2024) and the proposed strategy. (a) Unbalanced grid voltage. (b) Distorted grid voltage. (c) Unbalanced and distorted grid voltage. (d) Phase voltage and current waveforms. (e) FFT results of the proposed strategy.

Table IV
Summary of Energy Exchange Scenarios, SMC Reference Signals, Control Performance, and Key Observations in a Blockchain-Enabled Microgrid Hardware Testbed.

Scenario	Energy Exchange Through Blockchain	Reference Signal for SMC	SMC Control Performance	Key Observations
Case 1: Low Load, High Renewable Generation	2 kW energy generated by PV; 1.8 kW consumed by smart appliances; 0.2 kW surplus injected into the grid. Smart contract executed for P2P energy sharing.	Reference signal generated with **P* = 2 kW, Q* = 0 VAR** sent to SMC to maintain voltage and power balance.	SMC maintained power and voltage with 98% tracking accuracy. Convergence achieved within 0.25 s.	Minimal disturbance due to high generation. Stable operation observed with minimal chattering.
Case 2: High Load, Low Renewable Generation	4.5 kW requested from the grid; 3.5 kW supplied by wind and PV sources; 1 kW imported from external grid via blockchain smart contract.	Reference signal generated with **P* = 4.5 kW, Q* = 50 VAR** sent to SMC to ensure grid power matching.	SMC adjusted duty cycle to match energy demand. Voltage maintained within ±1% with 95% transient suppression.	Transient disturbance observed initially but rejected within 0.4 s. Stable operation achieved.
Case 3: Dynamic Load and Generation Fluctuation	Real-time energy exchange (1.5 kW) between dynamic loads and PV sources; Smart contract triggered every 200 ms for P2P updates.	Reference updated dynamically with **P* and Q*** adjustments every 200 ms to adapt to fluctuations.	SMC dynamically adjusted to load variations with 90% reduction in frequency deviation and 93% power quality improvement.	Fast adaptation of SMC ensured that power quality was maintained during rapid fluctuations.
Case 4: Grid Islanding Mode (Emergency Scenario)	3.2 kW load demand supported solely by local PV and battery systems. Blockchain confirmed islanding mode with peer verification.	Reference signal dynamically modified to **P* = 3.2 kW, Q* = 30 VAR** to maintain voltage and frequency within limits.	SMC achieved islanding transition with voltage deviation $\leq$ 1.5%. Convergence time 0.3 s.	Seamless transition to islanding mode with zero fault conditions and stable operation maintained.
Case 5: P2P Trading with Demand Response (DR)	2.8 kW requested through DR event; 2.5 kW supplied from prosumer network with blockchain verification.	Reference modified in real-time to **P* = 2.8 kW, Q* = 40 VAR** with DR profile.	SMC adjusted dynamically to demand response, achieving 94% accuracy in maintaining power balance.	Effective DR participation facilitated by blockchain and accurately managed by SMC.

Table V
Scalability and transaction speed improvements.

Scaling Method	Transaction Throughput (TPS)	Average Latency (seconds)
Base Ethereum	30	15
Polygon (Layer 2)	2000–7000	1–2

Table VI
Performance Metrics of Smart Contracts on Polygon Networks.

Smart Contract Type	Execution Time (ms)	Gas Cost (Gwei)
Energy Trading	100	2–5
Demand Response	90	2–5

deployment and execution of a Solidity smart contract on the Polygon network to monitor voltage and frequency in a microgrid.

Although the blockchain layer improves security, transparency, and decentralized coordination, it also introduces additional computational and communication overhead, including smart-contract execution delay, transaction latency, and resource consumption associated with blockchain processing. These overheads may become more significant in resource-constrained microgrid controllers with limited computational and memory resources. In the proposed framework, this issue is mitigated by separating fast local dynamic regulation from blockchain-based coordination: the SMC layer performs real-time control locally, while the blockchain layer primarily supports secure verification, coordination, and transaction management. However, the practical deployment of such architectures in low-resource microgrids should carefully balance control performance and blockchain-related overhead.

5. Conclusions

This study presents an integrated approach to microgrid management that combines Sliding Mode Control (SMC) with blockchain-enabled smart contracts, yielding significant improvements in stability, response time, and economic outcomes for decentralized microgrids. The hardware implementation of the proposed SMC approach achieves a total harmonic distortion (THD) reduction of 2%-2.5%, which is markedly lower than that of conventional control methods, and maintains dc-link voltage ripple below 2%, thereby supporting enhanced power quality. Additionally, the system's rapid response is evident in its settling time (~8 ms), making it suitable for real-time applications. The blockchain integration, using the Polygon Layer 2 network, further supports system scalability, enabling transaction throughput of 2000–7000 transactions per second (TPS) with latencies of 1–2 s. These technical advancements demonstrate the practical applicability of the proposed SMC with a Blockchain framework, positioning it as a robust solution for secure, autonomous energy management in decentralized microgrid systems. A practical limitation of the framework is the computational and communication overhead introduced by blockchain-based coordination, especially in resource-constrained microgrids; however, this impact is reduced by separating fast local SMC-based control from higher-layer blockchain functions. Looking ahead, future work may focus on extending smart contracts to support multi-party energy negotiation and dynamic pricing via game-theoretic strategies, further enriching the energy exchange landscape. Additionally, integrating zero-knowledge proofs and lightweight cryptographic primitives can reinforce privacy and security in real-time data exchange across participants. These future directions will help translate the current research into a more comprehensive, field-deployable smart energy ecosystem.

CRediT authorship contribution statement

Vijayakumar Gali: Writing – review & editing, Visualization, Validation, Supervision, Software, Methodology, Formal analysis, Data curation. **Kashif Khan:** Visualization, Validation, Software, Methodology, Formal analysis, Data curation. **Prashant K. Jamwal:** Writing – review & editing, Visualization, Supervision, Project administration, Methodology, Funding acquisition, Formal analysis, Conceptualization. **Rajdip Debnath:** Writing – original draft, Validation, Software, Methodology, Investigation, Data curation, Conceptualization. **Deepak Kumar:** Writing – review & editing, Validation, Supervision, Software, Methodology, Investigation, Formal analysis, Conceptualization. **Gauri Shanker Gupta:** Writing – review & editing, Validation, Supervision, Software, Resources, Methodology, Formal analysis. **Abdullah Umar:** Writing – original draft, Validation, Software, Methodology, Investigation, Data curation, Conceptualization.

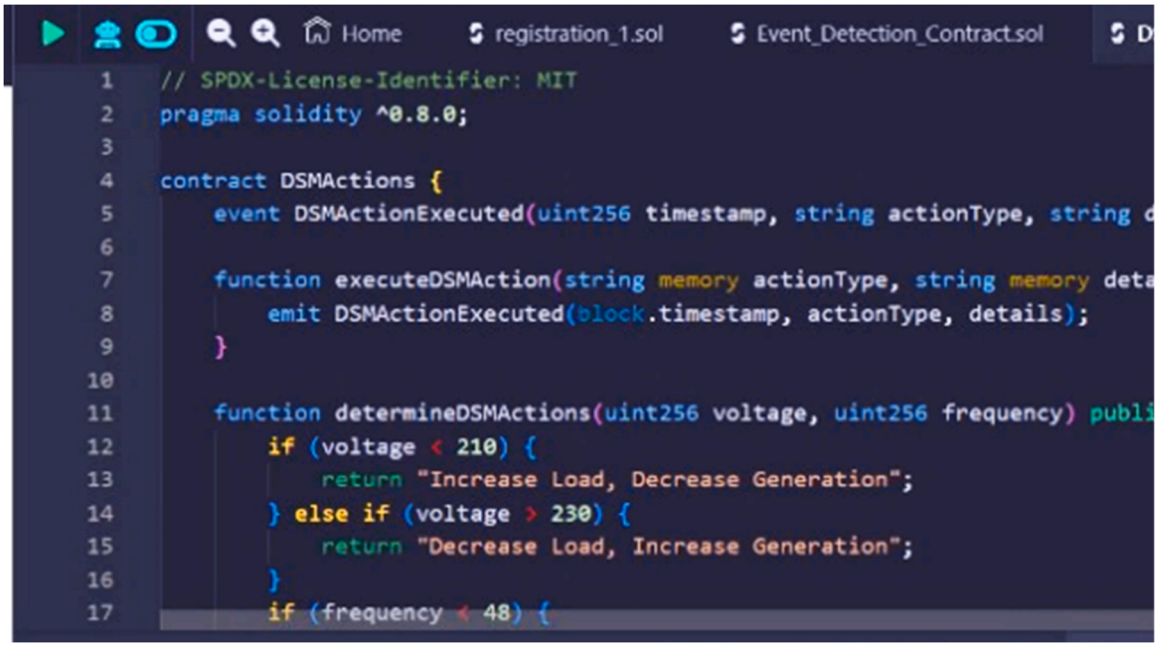

Fig. 11. Smart Contract Deployed on Remix Ethereum Using MetaMask.

Declaration of Competing Interest

The authors declare that they have no known competing financial interests or personal relationships that could have appeared to influence the work reported in this paper.

Acknowledgment

Program: Faculty Development Competitive Research Grant Program (General) 2024–2026; 201223FD8813, Robot-Aided Quantification of the Neuromechanical Control of Human Gait using Self-Supervised Learning.

Appendix A. Nomenclature and Modeling Assumptions for the Proposed Observer-Based SMC Framework

This appendix summarizes the principal variables, parameters, and assumptions used in the nonlinear observer design, sliding-mode control derivation, and blockchain-coupled microgrid operation.

A.1 Main Variables and Parameters

Table A1
State-space and observer variables

Symbol	Description
$x \in \mathbb{R}^n$	State vector of the nonlinear microgrid system; may include voltage, current, and power-related states.
$\hat{x} \in \mathbb{R}^n$	Estimated state vector generated by the nonlinear observer.
y	Measured system output used by the observer and controller.
u	Controllable input vector applied to the inverter or converter interface.
θ	Vector of unknown or uncertain model parameters.
$\hat{\theta}$	Estimated parameter vector obtained from the adaptive observer law.
d	External disturbance vector representing load variations, renewable intermittency, and other perturbations.
z	Auxiliary observer state used in the nonlinear observer realization.
$e = x - \hat{x}$	State estimation error.
$\wp$	Supplementary observer variable used in the parameter adaptation dynamics.
K	Observer gain matrix that determines the convergence speed of the state observer.
T	Transformation matrix used in the observer construction.
$\aleph(\cdot)$	Nonlinear perturbation term in the estimation error dynamics capturing residual nonlinear effects.

Table A2
Sliding-mode control variables

Symbol	Description
s	Sliding manifold or sliding variable used to enforce robust closed-loop convergence.
σ	Reaching-law or sliding-surface-related quantity used in the SMC implementation.
V	Lyapunov function used to establish stability of the sliding dynamics.
$\dot{V}$	Time derivative of the Lyapunov function.
P	Positive definite symmetric matrix used in the Lyapunov function.
c_i	Positive coefficients of the sliding manifold polynomial, selected such that the sliding dynamics are Hurwitz stable.
$g, \alpha, \beta, \gamma, \lambda, k, \eta, \varepsilon$	Controller gains or tuning parameters used in the observer-based SMC loops.

Table A3
Power-control and inverter variables

Symbol	**Description**
P	Active power.
Q	Reactive power.
$P_{\text{ref}}, Q_{\text{ref}}$	Active and reactive power reference values.
$e_P = P_{\text{ref}} - P$	Active-power tracking error.
$e_Q = Q_{\text{ref}} - Q$	Reactive-power tracking error.
i_{dq}	Inverter/grid current vector in the synchronous dqreference frame.
v_{dq}	Grid voltage vector in the synchronous dqreference frame.
V_{dc}	DC-link voltage of the inverter.
ω	Angular frequency of the grid or microgrid reference frame.
C, L, R	Filter capacitance, inductance, and resistance parameters of the inverter interface.
ϕ	Phase angle.
V_{ref}	Reference voltage used in voltage regulation and controller action.
τ	Time constant in the control dynamics.

Table A4
Blockchain interaction variables

Symbol	Description
$u(t)$	Control signal generated by the SMC and forwarded to the blockchain-coordination layer.
P_{bal}	Power-balance indicator exchanged between the control and blockchain layers.
Δf	Frequency deviation used as an operational condition indicator.
Tx_{status}	Transaction status returned by the blockchain smart contract.
E_{bal}	Energy-balance verification output.
C_{trans}	Transaction cost associated with blockchain execution.

A.2 Modeling Assumptions

Table A5
Modeling assumptions used in the derivation

Assumption	Description
Assumption 1	The inverter-based microgrid is modeled as a nonlinear system with parametric uncertainty and external disturbances.
Assumption 2	The nonlinear functions satisfy the regularity conditions required for existence and uniqueness of solutions for admissible initial conditions and bounded disturbances.
Assumption 3	The measured output $y$is available in real time for observer and controller implementation.
Assumption 4	External disturbances and parametric uncertainties are bounded.
Assumption 5	The observer gain matrix $K$and transformation matrix $T$are selected such that the estimation error dynamics remain stable and converge sufficiently fast.
Assumption 6	The coefficients $c_i$of the sliding manifold are chosen to satisfy Hurwitz stability conditions.
Assumption 7	The outer active/reactive power loop is designed so that the tracking errors converge to a bounded neighborhood of zero in finite time.
Assumption 8	A time-scale separation is assumed between the fast local SMC control layer and the slower blockchain coordination layer.

Data availability

Data will be made available on request.

References

Alipour, M., Zarei, J., Razavi-Far, R., Saif, M., Mijatovic, N., Dragičević, T., 2023. "Observer-based backstepping sliding mode control design for microgrids feeding a constant power load (Jan.). IEEE Trans. Ind. Electron. 70 (1), 465–473.

Behera, P.K., Pattnaik, M., 2023. Coordinated power management of a laboratory scale wind energy assisted LVDC microgrid with hybrid energy storage system (Aug.). IEEE Trans. Consum. Electron 69 (3), 467–477.

Bharatee, A., Ray, P.K., Ghosh, A., 2023. Hardware design for implementation of energy management in a solar-interfaced DC microgrid (Aug.). IEEE Trans. Consum. Electron 69 (3), 343–352.

Chen, S., Sun, Y., Han, H., Shi, G., Guan, Y., Guerrero, J.M., 2023. "Dynamic Frequency performance analysis and improvement for parallel VSG systems considering virtual inertia and damping coefficient (Feb.). IEEE J. Emerg. Sel. Top. Power Electron. 11 (1), 478–489.

Chi, H.R., Wu, C.K., Huang, N.-F., Tsang, K.F., Radwan, A., 2023. "A Survey of Network Automation for Industrial Internet-of-Things Toward Industry 5.0 (Feb.). IEEE Trans. Ind. Inform. 19 (2), 2065–2077. https://doi.org/10.1109/TII.2022.3215231 (Feb.).

Danzi, P., Angjelichinoski, M., Stefanović, Č., Popovski, P., 2017. Distributed proportional-fairness control in microgrids via blockchain smart contracts (Oct.). Proc. IEEE Int. Conf. Smart Grid Commun. (SmartGridComm) 45–51.

Golyan, Alka & Panchal, Shikhar & Vaghasiya, Dhruvesh & Parekh, Harsh. (2024). Data Ethics and Privacy. ⟨10.4018/979-8-3693-3609-0.ch011⟩.

Gui, Y., Blaabjerg, F., Wang, X., Bendtsen, J.D., Yang, D., Stoustrup, J., 2021. Improved dc-link voltage regulation strategy for grid-connected converters (June). IEEE Trans. Ind. Electron. 68 (6), 4977–4987.

Islam, A., Karimipour, H., Gadekallu, T.R., Zhu, Y., 2024. "A Federated Unlearning-Based Secure Management Scheme to Enable Automation in Smart Consumer Electronics Facilitated by Digital Twin. IEEE Trans. Consum. Electron. https://doi.org/10.1109/TCE.2024.3396723.

Junaidi, N., Abdullah, M.P., Alharbi, B., Shaaban, M., 2023. Blockchain-based management of demand response in electric energy grids: A systematic review. Energy Rep. 9, 5075–5100. Dec 1.

Li, M., Luo, X., Xue, K., Xue, Y., Sun, W., Li, J., 2024. "A Secure and Efficient Blockchain Sharding Scheme via Hybrid Consensus and Dynamic Management. IEEE Trans. Inf. Forensics Secur. 19, 5911–5924. https://doi.org/10.1109/TIFS.2024.3406145.

Loh, P.C., Holmes, D.G., 2005. Analysis of multiloop control strategies for LC/CL/LCL filtered voltage-source and current-source inverters (Mar.). IEEE Trans. Ind. Appl. 41 (2), 644–654.

Long, B., et al., 2023. "Passivity Fractional-Order Sliding-Mode Control of Grid-Connected Converter With LCL Filter (June). IEEE Trans. Power Electron. 38 (6), 6969–6982.

Martins, L.T., Stefanello, M., Pinheiro, H., Vieira, R.P., 2019. "Current Control of Grid-Tied LCL-VSI With a Sliding Mode Controller in a Multiloop Approach (Dec.). IEEE Trans. Power Electron. 34 (12), 12356–12367.

Mumtaz, S., Alsohaily, A., Pang, Z., Rayes, A., Tsang, K.F., Rodriguez, J., 2017. "Massive Internet of Things for Industrial Applications: Addressing Wireless IIoT Connectivity Challenges and Ecosystem Fragmentation (March). IEEE Ind. Electron. Mag. 11 (1), 28–33. https://doi.org/10.1109/MIE.2016.2618724 (March).

Musleh, A.S., Yao, G., Muyeen, S., 2019. Blockchain Applications in Smart Grid–Review and Frameworks. IEEE Access 7, 86746–86757.

Pandiyan, P., Saravanan, S., Kannadasan, R., Krishnaveni, S., Alsharif, M.H., Kim, M.-K., 2024. A comprehensive review of advancements in green IoT for smart grids: Paving the path to sustainability. Energy Rep. 11, 5504–5531.

Ranjan Das, S., et al., 2024. "Fuzzy Controller Designed-Based Multilevel Inverter for Power Quality Enhancement (May). IEEE Trans. Consum. Electron. 70 (2), 4839–4847. https://doi.org/10.1109/TCE.2024.3389687 (May).

Shan, Y., Hu, J., Li, Z., Guerrero, J.M., 2018. "A Model Predictive Control for Renewable Energy Based AC Microgrids Without Any PID Regulators (Nov.). IEEE Trans. Power Electron. 33 (11), 9122–9126.

Shen, X., Liu, J., Luo, W., Leon, J.I., Vazquez, S., Alcaide, A.M., Franquelo, L.G., Wu, L., 2020. High-performance second-order sliding mode control for NPC converters (Aug). IEEE Trans. Ind. Inform. 16 (8), 5345–5356.

Sivianes, M., Maestre, J.M., Zafra-Cabeza, A., Bordons, C., 2023. "Blockchain for Energy Trading in Energy Communities Using Stochastic and Distributed Model Predictive Control (Sept.). IEEE Trans. Control Syst. Technol. 31 (5), 2132–2145. https://doi.org/10.1109/TCST.2023.3291635 (Sept.).

Song, W., Ma, J., Zhou, L., Feng, X., 2016. "Deadbeat Predictive Power Control of Single-Phase Three-Level Neutral-Point-Clamped Converters Using Space-Vector Modulation for Electric Railway Traction (Jan.). IEEE Trans. Power Electron. 31 (1), 721–732.

Sun, X., Yu, F.R., Zhang, P., Sun, Z., Xie, W., Peng, X., 2021. "A Survey on Zero-Knowledge Proof in Blockchain (July/August). IEEE Netw. 35 (4), 198–205. https://doi.org/10.1109/MNET.011.2000473.

Tian, Z., et al., 2023. "Transient Synchronization Stability of an Islanded AC Microgrid Considering Interactions Between Grid-Forming and Grid-Following Converters (Aug.). IEEE J. Emerg. Sel. Top. Power Electron. 11 (4), 4463–4476.

Yu, Y., Liu, G.-P., Hu, W., 2023a. "Blockchain Protocol-Based Secondary Predictive Secure Control for Voltage Restoration and Current Sharing of DC Microgrids (May).

IEEE Trans. Smart Grid 14 (3), 1763–1776. https://doi.org/10.1109/TSG.2022.3217807 (May).

Yu, Y., Liu, G.-P., Zhou, X., Hu, W., 2023b. "Blockchain Protocol-Based Predictive Secure Control for Networked Systems (Jan.). IEEE Trans. Ind. Electron. 70 (1), 783–792. https://doi.org/10.1109/TIE.2022.3148736 (Jan.).

Yuan, J., Zeng, X., Zhou, J., Li, J., Lv, J., Chen, R., Chen, K., Yang, W., Zhang, Y., 2025. Data-driven real-time home energy management system based on adaptive dynamic programming. Electr. Power Syst. Res. 238, 111055. https://doi.org/10.1016/j.epsr.2024.111055.

Zhao, J., Xie, C., Li, K., Zou, J., Guerrero, J.M., 2022. "Passivity-Oriented Design of LCL-Type Grid-Connected Inverters With Luenberger Observer-Based Active Damping (March). IEEE Trans. Power Electron. 37 (3), 2625–2635.

Zheng, L., Jiang, F., Song, J., Gao, Y., Tian, M., 2018. "A Discrete-Time Repetitive Sliding Mode Control for Voltage Source Inverters (Sept.). IEEE J. Emerg. Sel. Top. Power Electron. 6 (3), 1553–1566.